

# Experimental Evaluation of an Analytically Derived Bleed System for a Supersonic Inlet

Jan Syberg\* and Joseph L. Koncsek†  
The Boeing Company, Seattle, Wash.

Wind tunnel test results for a large-scale Mach 3.5 inlet model featuring an analytically derived bleed system are compared with flowfield and boundary-layer predictions. The high performance achieved at the design Mach number indicates that boundary-layer bleed requirements can be accurately predicted. The highest engine-face recovery at Mach 3.5 was 85.8%; this was obtained at 0.05 Mach tolerance with 13.4% bleed. In the "started" Mach number range from 1.6 to 3.5, the total-pressure recovery in the throat, downstream of the terminal normal shock, ranged between 91% and 95%. Subsonic-diffuser losses were significant at some off-design Mach numbers.

## Nomenclature

$A/A^*$	= sonic area ratio
$A_L$	= cowl lip area = 0.1942 m <sup>2</sup>
$d$	= bleed hole diameter
$H$	= boundary-layer shape factor
$M$	= freestream Mach number
$P$	= static pressure
$P_P$	= pitot pressure
$P_T$	= total pressure
$P_{TAV}$	= area weighted average total pressure at engine face
$P_{To}$	= freestream total pressure
$R_L$	= cowl lip radius = 24.86 cm
$V_\infty$	= freestream velocity
$W$	= mass flow
$W_L$	= lip mass flow, $\rho_\infty V_\infty A_L$
$X$	= inlet station, referenced to tip of centerbody in design position
$X_{CB}$	= centerbody station, referenced to tip of centerbody
$\Delta X/R_L$	= forward translation of the centerbody from the design position normalized to the lip radius
$\delta^*$	= boundary-layer displacement thickness
$\rho_\infty$	= freestream density
<i>Subscript</i>	
TH	= throat

## Introduction

THE development of bleed systems for boundary-layer control in supersonic inlets in the past depended mainly on extensive wind tunnel tests. The tests were complex and time consuming and did not always allow optimization of the system. An analytical procedure has been developed for the design of bleed systems based on theoretical analysis and extensive experimental data. Using the procedure allows analytical definition of a bleed system, which may then be optimized in the wind tunnel with less testing.

This procedure was recently applied to the design of a bleed system for a Mach 3.5 inlet with the objective of providing satisfactory operation across a wide range of "started" Mach numbers with adequate tolerance to transient disturbances in

Presented as Paper 75-1210 at the AIAA/SAE 11th Propulsion Conference, Anaheim, Calif., September 29-October 1, 1975; submitted September 26, 1975; revision received December 1, 1975.

Index category: Airbreathing Propulsion, Subsonic and Supersonic.

\*Senior Specialist Engineer.

†Specialist Engineer.

upstream Mach number and angle of incidence and in downstream corrected airflow. The work included the design of internal cowl and centerbody contours, design of the bleed pattern, bleed hole geometry, bleed plenum arrangement, bleed flow ducting and exits, and the prediction of bleed system performance. The inlet and bleed system were sized for an existing large-scale supersonic inlet model operating in the flow environment in the NASA-Ames 8 by 7 ft supersonic wind tunnel. This work was carried out under contract NAS2-6643 and is described in detail in Ref. 1.

This application of the procedure was the first time a completely analytical design of the bleed system had been done prior to model testing. A thorough validation of the procedures was therefore needed from wind tunnel tests of the inlet. This paper summarizes the results from a test conducted in the NASA-Ames Unitary Plan Wind Tunnels with a large-scale model of the Mach 3.5 inlet. Comparisons of test data and analytical predictions are included.

The test program was sponsored by the NASA-Ames Research Center under contract NAS2-8236. A comprehensive analysis of the data is published in Ref. 2.

## Inlet and Bleed System Design

The inlet, Fig. 1, is an axisymmetric, mixed-compression type and uses a translating centerbody for throat area variation. At the design Mach number, the centerbody is in the fully retracted position ( $\Delta X/R_L = 0$ ), providing a capture mass-flow ratio of unity. During operation at lower Mach numbers, the centerbody translates forward, thereby increasing the throat area to maintain the desired throat Mach number.

For transonic operation, the centerbody is extended forward to position the maximum diameter of the centerbody near the cowl lip station, creating a minimum flow area at this

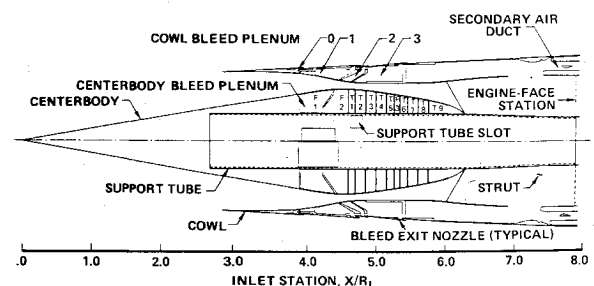


Fig. 1 Mach 3.5 inlet model schematic.

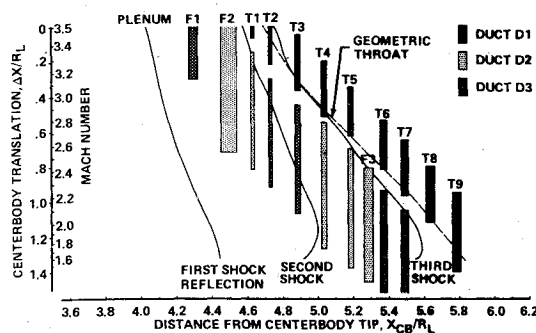


Fig. 2 Centerbody bleed schedule.

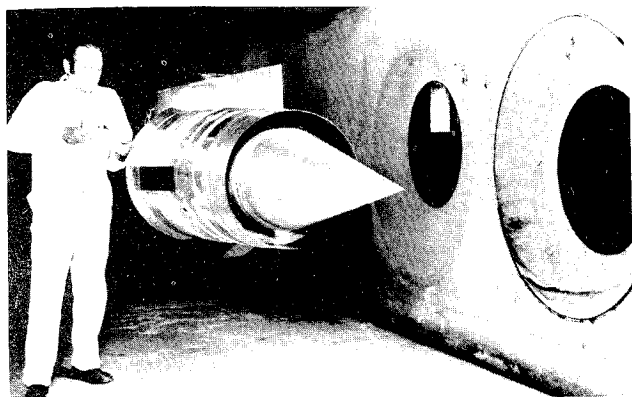


Fig. 3 Mach 3.5 inlet model installed in wind tunnel.

station. One design objective was to develop an inlet with large transonic flow capacity without using auxiliary airflow devices such as collapsible centerbody, throat doors, or external cowl scoops. This leads to an inlet with high cowl compression and a relatively small centerbody. Furthermore, the translation required in such an inlet is usually longer than in an inlet with less transonic flow capacity. For the present inlet, the transonic flow area is 42.4% of the cowl lip area.

As the centerbody is retracted from the transonic position, a minimum flow area is formed farther downstream. The inlet can then be operated in the mixed-compression started mode. For this mode, the location of the inlet throat remains fixed on the cowl and thus moves forward on the centerbody when the centerbody translates aft for operation at increasing Mach numbers. Experience has shown that bleed is required in the throat region on both surfaces to adequately control the normal shock/boundary-layer interaction. A traveling centerbody bleed system featuring 12 bleed plenums coupled with a triple slot arrangement on the support tube (see Fig. 1) was designed after a detailed analytical study of the bleed requirements at  $M=3.5$  and selected off-design Mach numbers. This traveling system provides bleed in the throat as well as near the oblique shock reflections in the supersonic diffuser throughout the started-mode Mach number range of 1.6 to 3.5. Figure 2 illustrates the centerbody bleed schedule.

The design of the cowl bleed system is considerably different from that of the centerbody system. A traveling bleed is not necessary, as the supersonic diffuser always occupies essentially the same portion of the cowl contour. Four bleed plenums are used, each with its own bleed plenum exit. The first three plenums provide forward bleed removal, and the fourth acts as throat bleed.

The boundary-layer bleed systems were developed using analytical procedures based on method-of-characteristic solutions of supersonic stream flows and finite-difference calculations of boundary-layer development. Empirical coefficients were used in modeling the boundary-layer control systems. The analytical predictions of boundary-layer

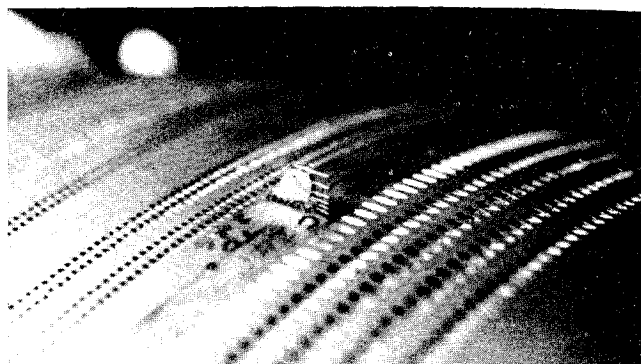


Fig. 4 Typical boundary-layer rake installation.

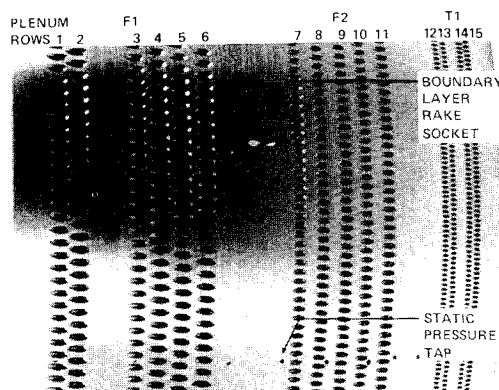


Fig. 5 Centerbody bleed holes.

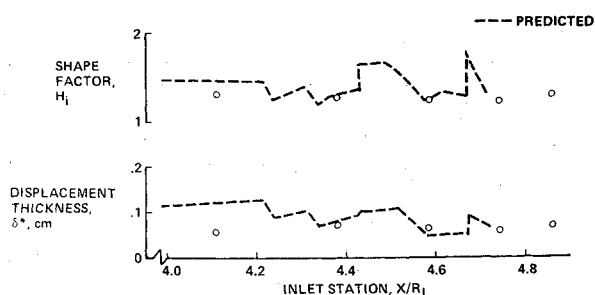
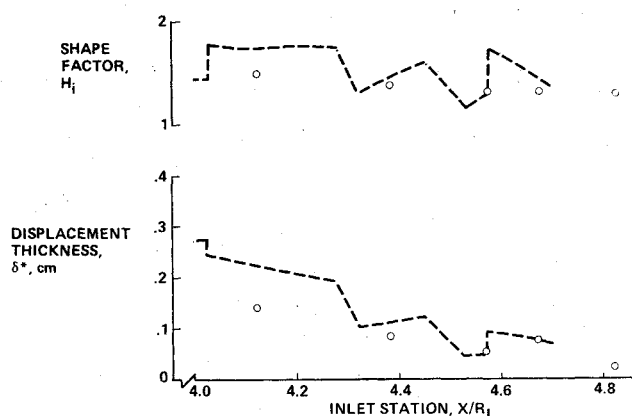
development and required bleed flow rates were limited to the supersonic diffuser. The normal-shock/boundary-layer interactions are beyond the capabilities of the current analysis. Throat bleed rates were selected on the basis of past experience with axisymmetric supersonic inlets.

### Test Apparatus

The 49.72-cm lip diameter inlet model was tested in the NASA-Ames Unitary Plan Wind Tunnels, Fig. 3, at freestream Mach numbers from 0.6 to 3.5. The corresponding Reynolds numbers, based on cowl lip diameter, ranged from  $2.8 \times 10^6$  at  $M=3.5$  to about  $7.0 \times 10^6$  at the transonic and subsonic Mach numbers. The inlet was coupled to a sting-mounted flow duct assembly with a variable plug valve at the aft end to simulate the flow demand of a jet engine.

The model instrumentation consisted of pitot-pressure rakes and surface static taps. A total of 366 steady-state pressures were recorded for each data point. Of fundamental importance in comparing the test results to analytical predictions were the data obtained with 10 boundary-layer rakes distributed along the cowl and the centerbody surfaces. The probes were made of 0.025-cm inside diameter tubing. The inner three probes were flattened to 0.01-cm inside dimension to improve the accuracy of measurement in the high-velocity-gradient part of the boundary layer near the surface. Figure 4 shows a typical rake installation.

The model was provided with a large number of bleed holes to obtain the desired bleed rates throughout the started Mach number range. All centerbody bleed holes and the forward cowl bleed holes were slanted  $20^\circ$  with respect to the local surface to maximize the bleed plenum pressure. The cowl throat bleed holes were normal to the surface to provide maximum normal shock stability. A photograph of some of the centerbody bleed holes is shown in Fig. 5. This figure illustrates the typical variation of hole diameter to obtain the desired flow area and hole spacing in each region as well as to keep

Fig. 6 Cowl boundary-layer development,  $M=3.5$ .Fig. 7 Centerbody boundary-layer development,  $M=3.5$ .

the hole diameter small with respect to the predicted boundary-layer thickness ( $d \approx \delta^*$ ). The bleed hole diameter ranged from 0.066 to 0.159 cm.

### Supersonic Diffuser Performance

The primary objective of the test program was to verify the analytical procedures used in the design of the supersonic diffuser. Comparisons of data with analytical predictions are presented in this section. For these data, the inlet normal shock is located far downstream of the throat in order not to obscure the performance of the supersonic diffuser. Test results obtained with the normal shock at or near the critical position are presented in a later section.

#### Boundary-Layer Development

The theoretical and experimental boundary-layer development is shown in Fig. 6 for the cowl and in Fig. 7 for the centerbody at the design Mach number. The boundary-layer properties are shown in terms of displacement thickness  $\delta^*$  and shape factor  $H_i$ . An  $H_i$  of about 1.3 corresponds to a "full" velocity profile (similar to a one-seventh power law profile), while an  $H_i$  between 1.8 to 2.0 indicates a highly distorted profile close to separation. The data show that the boundary layer is well controlled with the analytically designed bleed system, and the goal of providing a full profile in the inlet throat is achieved on both surfaces. Thus, the boundary layer should be able to withstand the pressure rise from the normal shock without severe flow separation. This hypothesis is verified in a later section.

Note in Figs. 6 and 7 that the boundary-layer properties are evidently predicted somewhat conservatively in the upstream portion of the diffuser, whereas good agreement is observed farther downstream. The discrepancies at rake 1 are not fully understood but may be due to incorrect prediction of the point of transition coupled with an oversimplified modeling of the transition region.

The inlet model was tested in 0.10 Mach number increments between  $M=1.6$  and  $M=3.5$  to obtain a detailed comparison

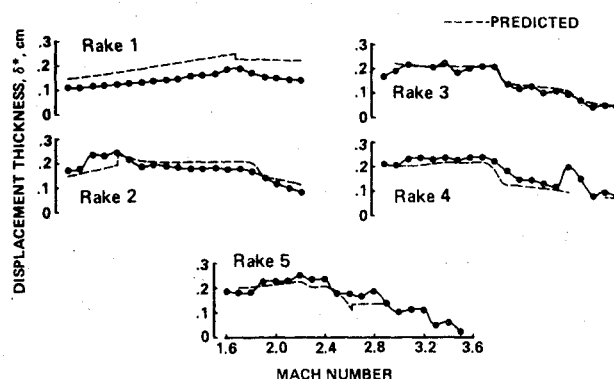


Fig. 8 Centerbody boundary-layer displacement thickness.

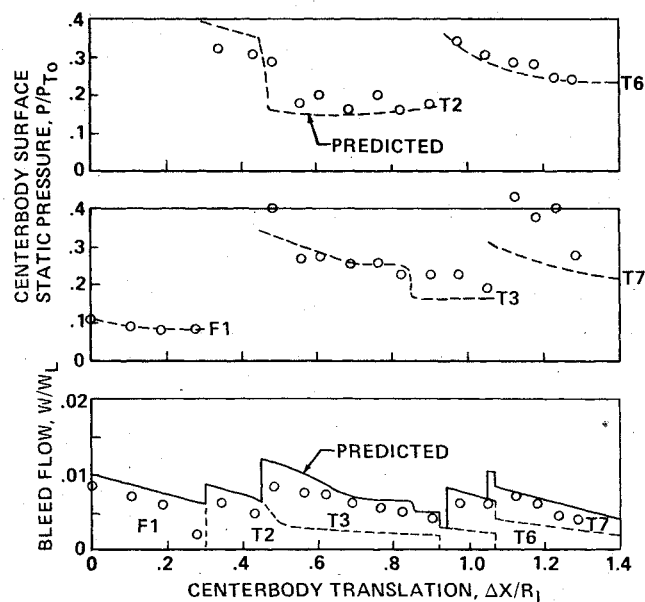


Fig. 9 Bleed rates and surface static pressures, support-tube duct D1.

with the analytical predictions. Figure 8 shows the centerbody boundary-layer displacement thicknesses at the five rakes vs inlet Mach number. The boundary layer is evidently well predicted throughout the Mach number range except for the conservative prediction at rake 1 as discussed earlier.

#### Bleed System Performance

Since the boundary-layer development is strongly dependent on the bleed system, the preceding comparison is meaningful only when combined with a comparison of measured and predicted bleed rates. The bleed flow requirements were determined from the analytical boundary-layer development. Predictions of bleed area requirements were based on the analytical inviscid surface static pressures and empirical bleed hole flow coefficients. Differences between theoretical and experimental bleed rates can be caused by differences in the surface static pressures as well as differences in the flow coefficients. To evaluate the bleed system performance, it is therefore necessary to examine the local surface static pressures across the individual bleed regions as well as the individual bleed flow rates. This is done in Fig. 9 for one of the forward bleed ducts in the centerbody bleed system. The data are shown vs centerbody position rather than Mach number to facilitate correlation with the centerbody bleed schedule in Fig. 2. (The freestream Mach number corresponding to a given centerbody position can also be obtained from Fig. 2). It is evident from Fig. 9 that the surface pressures for the individual bleed plenums in general are well predicted. The largest discrepancy occurs for plenum T7

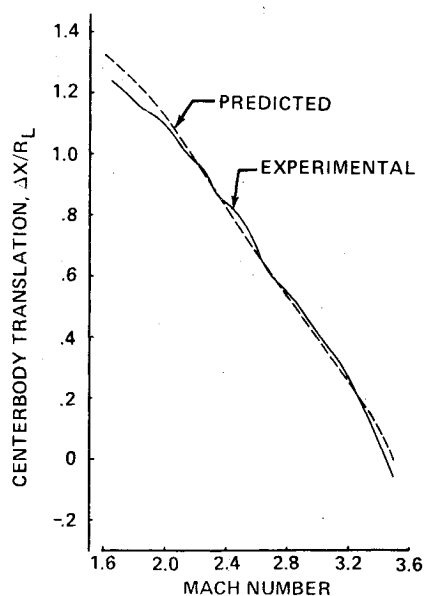


Fig. 10 Centerbody translation schedule. Comparison of theory with experiment.

because the third shock interaction has moved forward of the inviscid shock (see Fig. 2) influencing the pressure on T7. The bleed rates follow the predicted trend but are generally 10% to 20% lower, indicating that the bleed hole flow coefficients are lower than expected. The large discrepancy observed at  $\Delta X/R_L = 0.28$  ( $M = 3.2$ ) is due to internal bleed duct choking because the opening between the bleed plenum and the support tube duct is too small at this centerbody position to pass the choked bleed hole flow from plenum Fl.<sup>2</sup>

#### Supersonic Diffuser Efficiency

The inlet is designed to maintain a nominal throat Mach number of 1.25. As the freestream Mach number is decreased, the centerbody must translate forward to meet this requirement. A theoretical translation schedule was established during the analytical design of the inlet, and all predictions were made using this schedule. The centerbody schedule was derived simply by using the throat Mach numbers from the inviscid method-of-characteristic program and by assuming that the decrease in throat flow rate due to removal of bleed flow in the supersonic diffuser just compensates for the reduction in throat area due to boundary-layer blockage. This rule of thumb was quite accurate when applied to lower cruise Mach number inlets.<sup>3,4</sup> Consequently, for the present inlet, the theoretical centerbody schedule was used as a baseline by which to judge the supersonic diffuser performance.

The experimental centerbody translation schedule for operation with a throat Mach number of 1.25 was established by first determining the critical centerbody positions (inlet unstart) at each Mach number and then adding 0.05 Mach number to the critical schedule. For example, if the inlet unstarts at  $\Delta X/R_L = 0.90$  at  $M = 2.25$ , then the throat Mach number will be about 1.25 at  $M = 2.30$  and  $\Delta X/R_L = 0.90$ , because

$$\frac{(A/A_*)_{M=2.30}}{(A/A_*)_{M=2.25}} = \frac{2.193}{2.096} = 1.047 = (A/A_*)_{M=1.25} \quad (1)$$

It is assumed here that the inlet throat flow ratio ( $W_{TH}/W_L$ ) and throat recovery remain unchanged while increasing the freestream Mach number from 2.25 to 2.30. In addition, it is assumed that the inlet unstart at the critical  $\Delta X/R_L$  occurs as a result of inlet choking ( $M_{TH} = 1.0$ ) rather than because of sudden boundary-layer separation that can reduce the effective throat area.

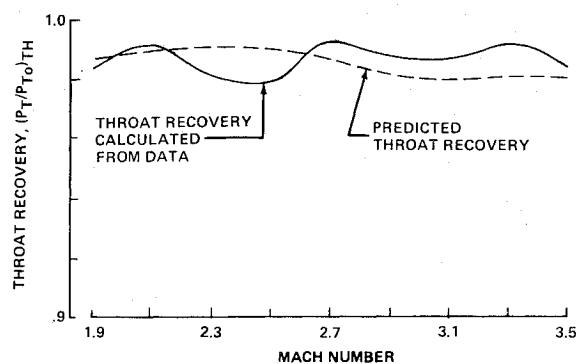


Fig. 11 Supersonic diffuser efficiency.

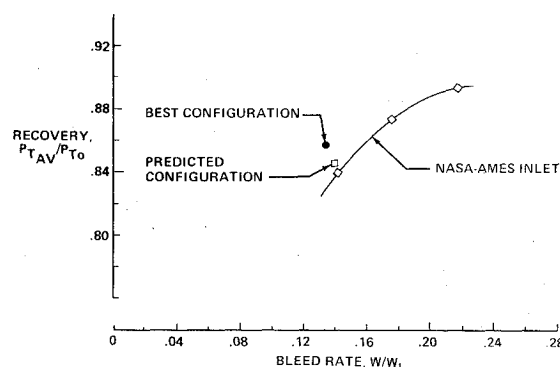


Fig. 12 Critical performance at  $M = 3.5$ .

The theoretical and experimental translation schedules are compared in Fig. 10. The fact that the inlet can be operated on or inside the design schedule with a throat Mach number of 1.25 indicates that there are no severe boundary-layer separations in the supersonic diffuser. Further, with a well-controlled boundary layer, the strengths of the oblique shocks should be close to the theoretical inviscid strengths, and the total-pressure losses in the supersonic diffuser then should be close to the predicted losses.

The throat total-pressure recovery can be computed if the throat flow ratio, the throat blockage, and the throat Mach number are known. Since the measured boundary-layer properties are close to the predicted values,<sup>2</sup> it is reasonable to use the predicted throat blockage. The throat Mach numbers can be determined fairly accurately by an examination of the static pressures on the cowl and centerbody in the throat region with the normal shock at a supercritical position. Figure 11 shows that the throat total-pressure recovery thus computed agrees well with the predicted recovery, indicating that the actual oblique shock losses are close to the theoretical inviscid shock losses. Note that an increase in the throat blockage (i.e., reduction in effective throat area) requires an increase in total pressure to pass the same mass flow through the throat at the same throat Mach number. Therefore, Fig. 11 also confirms that the experimental boundary-layer blockage cannot be much greater than predicted, since the throat total pressure is already 98% to 99% of the freestream total pressure.

#### Started-Mode Inlet Performance

The performance of the inlet with the terminal normal shock located in the throat region (near the critical position) was evaluated throughout the started Mach number range. Various configuration changes were made to identify the significant parameters governing the inlet behavior, to determine the accuracy of analytical predictions, and to upgrade performance. Highlights of these studies are presented in the following paragraphs.

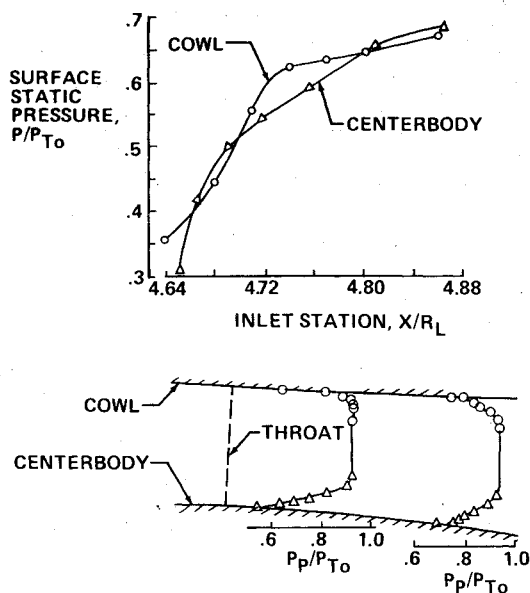
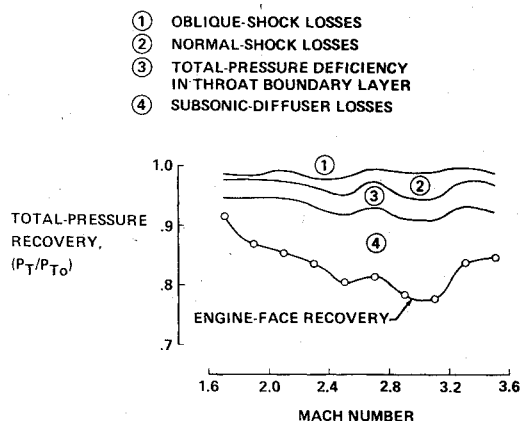
Fig. 13 Inlet throat profiles, best configuration,  $M=3.5$ .

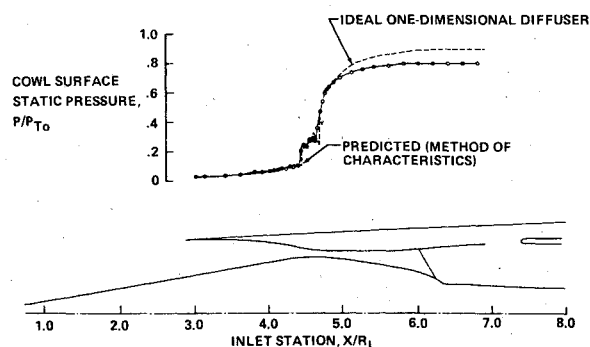
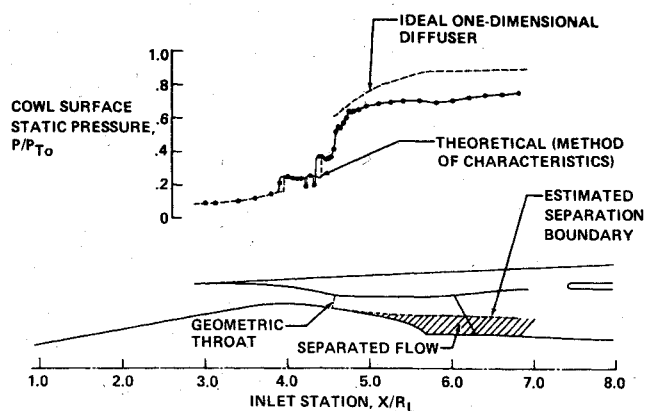
Fig. 14 Total-pressure losses.

#### Design Point Performance

It was shown in Figs. 6 and 7 that the predicted bleed configuration provided good boundary-layer control with full profiles in the throat at the design Mach number. The corresponding engine-face recovery with the normal shock at critical (i.e., just before unstart) is compared in Fig. 12 to that obtained by NASA on another inlet designed for  $M=3.5$ .<sup>5</sup> To our knowledge, the NASA inlet was the highest performance inlet previously tested at this Mach number. It is significant that the present inlet performed better than the NASA inlet at the design point with the analytically predicted bleed configuration demonstrating the validity and usefulness of the analytical design process. As shown in Fig. 12, the performance was later slightly improved by a minor change in bleed distribution and by the addition of centerbody vortex generators. Static and total-pressure profiles in the throat region at the critical point are presented in Fig. 13. The normal-shock/boundary-layer interaction is well controlled as indicated by the distinct pressure rise and the attached boundary-layer profiles downstream.

#### Off-Design Performance

The engine-face performance was expected to gradually increase with decreasing freestream Mach number, particularly since the supersonic diffuser boundary layer appeared to be well controlled. However, around  $M=3.2$ , the recovery suddenly decreased from about 85% to 78%. Below  $M=3.2$ , the recovery increased nearly linearly to 91% at  $M=1.6$ .

Fig. 15 Cowl static-pressure distributions,  $M=3.5$ .Fig. 16 Estimated separation boundary in subsonic diffuser,  $M=2.7$ .

To gain a better understanding of the aerodynamic efficiency of the inlet, the magnitudes of the total-pressure losses attributable to the various sources were estimated. The loss mechanisms were identified as: 1) supersonic diffuser oblique shocks; 2) terminal normal shock; 3) supersonic-diffuser boundary layer; and 4) subsonic diffusion, including boundary-layer and mixing losses. The results of the study are summarized in Fig. 14. The oblique-shock losses were determined through the method discussed in connection with Fig. 11. The normal-shock losses were computed using the experimental throat Mach numbers. The boundary-layer total-pressure deficiency just downstream of the normal shock was calculated from the measured pitot-pressure profiles at  $M=3.5$ . At off-design Mach numbers, the boundary-layer losses were assumed to be proportional to the estimated blockage values.

Subtracting the measured engine-face recovery from the subsonic-diffuser entry recovery, as derived from the preceding cumulative losses, yields the total-pressure losses in the subsonic diffuser (identified as region 4 in Fig. 14). It is evident that between  $M=1.7$  and  $M=3.2$ , the majority of the inlet total-pressure losses occur in the subsonic diffuser (i.e., downstream of the terminal normal shock). Such large losses could originate only in regions of separated flow in the subsonic diffuser. The engine-face total-pressure rakes indicated that the separations occurred on the centerbody while the flow on the cowl was attached. Figures 15 and 16 were prepared to estimate the spatial extent of the separations. In these figures, the experimental static-pressure distributions are compared with values calculated for an ideal one-dimensional diffuser using the experimental entry conditions and geometric area progressions. At  $M=3.5$  (Fig. 15), the experimental pressures initially approximate the ideal distribution and gradually deviate from it farther downstream as would be expected because of boundary-layer growth. At  $M=2.7$  (Fig. 16), the experimental pressures deviate significantly from the ideal distribution, indicating that the flow boundaries do not coin-

cide with the model surfaces. The aerodynamic area progression was calculated from the experimental static and estimated total-pressure distributions. The corresponding flow boundary is shown in the sketch in Fig. 16. The size of the separation calculated in this manner agrees with that indicated by the engine-fact total-pressure rakes.

The  $M=2.7$  case is typical of the off-design operation of the inlet in that high recovery and good boundary-layer properties are obtained up to the terminal normal shock followed by flow separation on the centerbody in the subsonic diffuser. Several centerbody vortex generator configurations were tested in an attempt to alleviate the separation, but no improvement was obtained. The problem appears to be caused by initially rapid area growth in the diffuser when the centerbody is translated forward for off-design operation as discussed in Ref. 2. Increasing the centerbody throat bleed and improving the off-design area progression at the expense of losing some of the transonic flow area would most likely eliminate the diffuser separation problem.

### Concluding Remarks

An axisymmetric mixed-compression inlet was designed for a cruise Mach number of 3.5 by applying an analytical design procedure. A large-scale model of the inlet was tested in the NASA-Ames Unitary Plan Wind Tunnels from  $M=0.6$  to  $M=3.5$ . The test results showed overall agreement with design predictions of the flowfield structure and boundary-layer development in the supersonic diffuser. In general, the bleed rate requirements were accurately predicted, but the actual bleed flow rates were accurately predicted, but the actual bleed flow rates were lower than predicted by about 20%.

The design point performance of the inlet was compared with that of the NASA model reported in Ref. 5. Both inlets were designed for about 98.5% inviscid total-pressure recovery in the throat. It is significant that the initial bleed configuration on the present inlet provided higher critical design point recovery than obtained on the NASA inlet with the same bleed flow rate, demonstrating the validity of the analytical design procedures.

In the started Mach number range, the total-pressure recovery downstream of the terminal normal shock exceeded 90% of the freestream total pressure. Significant total-pressure losses occurred in the subsonic diffuser below  $M=3.2$ , presumably caused by the initial rapid increase in diffuser area just downstream of the throat, possibly coupled with inadequate centerbody throat bleed.

### References

- <sup>1</sup>Syberg, J. and Hickcox, T.E., "Design of a Bleed System for a Mach 3.5 Inlet," NASA CR-2187, Jan. 1973.
- <sup>2</sup>Syberg, J. and Konesek, J.L., "Experimental Evaluation of a Mach 3.5 Axisymmetric Inlet," NASA CR-2563, July 1975.
- <sup>3</sup>Syberg, J. and Konesek, J.L., "Transonic and Supersonic Test of the SST Prototype Air Intake," Federal Aviation Administration, Washington, D.C., Rept. FAA-SS-72-50, April 1972.
- <sup>4</sup>Konesek, J. L. and Syberg, J., "Transonic and Supersonic Test of a Mach 2.65 Mixed-Compression Axisymmetric Intake, NASA CR-1977, March 1972.
- <sup>5</sup>Smeltzer, D. B. and Sorensen, N. E., "Investigation of a Mixed-Compression Axisymmetric Inlet System at Mach Numbers 0.6 to 3.5," NASA TN D-6078, No. 1970.

*From the AIAA Progress in Astronautics and Aeronautics Series . . .*

## AEROACOUSTICS: JET AND COMBUSTION NOISE; DUCT ACOUSTICS—v. 37

*Edited by Henry T. Nagamatsu, General Electric Research and Development Center; Jack V. O'Keefe, The Boeing Company; and Ira R. Schwartz, NASA Ames Research Center*

*A companion to Aeroacoustics: Fan, STOL, and Boundary Layer Noise; Sonic Boom; Aeroacoustic Instrumentation, volume 38 in the series.*

This volume includes twenty-eight papers covering jet noise, combustion and core engine noise, and duct acoustics, with summaries of panel discussions. The papers on jet noise include theory and applications, jet noise formulation, sound distribution, acoustic radiation refraction, temperature effects, jets and suppressor characteristics, jets as acoustic shields, and acoustics of swirling jets.

Papers on combustion and core-generated noise cover both theory and practice, examining ducted combustion, open flames, and some early results of core noise studies.

Studies of duct acoustics discuss cross section variations and sheared flow, radiation in and from lined shear flow, helical flow interactions, emission from aircraft ducts, plane wave propagation in a variable area duct, nozzle wave propagation, mean flow in a lined duct, nonuniform waveguide propagation, flow noise in turbofans, annular duct phenomena, freestream turbulent acoustics, and vortex shedding in cavities.

541 pp., 6 x 9, illus. \$19.00 Mem. \$30.00 List

TO ORDER WRITE: Publications Dept., AIAA, 1290 Avenue of the Americas, New York, N. Y. 10019